Measuring interface strains at the atomic resolution in depth using x-ray Bragg-surface diffraction

W. C. Sun, H. C. Chang, B. K. Wu, Y. R. Chen, C. H. Chu, and S. L. Chang[a)]
Department of Physics, National Tsing Hua University, Hsinchu 300, Taiwan, Republic of China

M. Hong
Department of Materials Science and Engineering, National Tsing Hua University, Hsinchu 300, Taiwan, Republic of China

M. T. Tang and Yu. P. Stetsko
National Synchrotron Radiation Research Center, Hsinchu 300, Taiwan, Republic of China

(Received 24 April 2006; accepted 10 July 2006; published online 31 August 2006)

A generic x-ray diffraction method, using three-wave Bragg-surface diffraction, is developed to measure strains at the interface of molecular beam epitaxial Au/GaAs(001), where grazing-incidence diffraction cannot be applied due to the difference in refractive index between Au and GaAs. Changes in diffraction images of the surface reflection (1−13) of GaAs(006)/(1−13) three-wave Bragg-surface diffraction and the (−1−13) of GaAs(006)/(−1−13) at different azimuth and Bragg angles give the depth penetration of 2 Å resolution and variations of lattice constant, −49%, −27%, and 2%, along the surface normal [001] and in-plane directions [−1−10] and [1−10] within the depths of 18, 72, and 72 Å, respectively. © *2006 American Institute of Physics*. [DOI: 10.1063/1.2345023]

Preparation of nanostructures, such as thin films, quantum dots, quantum wires, and superlattices on crystal substrates, has become an indispensable way of tailoring and producing materials for various electronic, photonic, mechanical, magnetic, chemical, and biological applications.[1–10] The strain induced at interfaces may deteriorate material properties due to crystal lattice distortion, thus degrading the performance and lifetime of the devices fabricated. Methods for characterizing interface strain are therefore most desired. Although many x-ray[4–17] and electron[18,19] diffraction techniques can be used to determine strains of thin films and crystals, probing strain at/near a buried interface under an overlayer film is yet very difficult. For the grazing-incidence diffraction[11–15] frequently employed for surfaces/interfaces, x rays scattered from the interface may be overshadowed by that diffracted from the substrate due to the large x-ray penetration depth. Moreover, when the refractive index of a thin film is smaller than that of the substrate, external total reflection does not occur for x rays traveling through the interface of the thin film and substrate. Without the totally reflected beam, the information about the interface structure may not be easily extracted from the intensity measurement of the transmitted diffracted beam.[16] To overcome this difficulty, we propose a method to determine three-dimensional interface strain nondestructively with an atomic resolution for the molecular beam epitaxial (MBE) Au/GaAs(001) sample system where the refractive index of gold is smaller than that of GaAs for x rays. No total external reflection occurs unless diffraction takes place from the back side of the sample.[16] The proposed method adopts the so-called Bragg-surface multiple diffraction (BSD),[4,20] where a surface diffracted wave carries interface structural information.

The sample is a 170 Å thick (110) gold film on a GaAs (001) surface prepared by MBE.[5] The crystal size is 15 $\times$ 15 mm^2. The crystallographic orientation of the Au film relative to the substrate GaAs is determined. The lattice mismatches of Au along [00−1] and [−1−10] are 2% and 27% with respect to that along [1−10] and [−110] of GaAs, where the lattice constant is 4.078 Å for single-crystal Au and 5.6539 Å for GaAs. This sample system is ideal for demonstrating this diffraction method for interface investigation, because of the anisotropic lattice mismatch between the two materials and the refractive index of gold being smaller than that of GaAs for x rays.

X-ray Bragg-surface diffraction measurements were conducted at the wiggler beamline BL17B, the National Synchrotron Radiation Research Center (NSRRC). A Si(111) double-crystal monochromator and a collimating mirror provided a highly monochromatic ($\Delta E/E \sim 10^{-4}$) and collimated beam. The x-ray energy used was 11.0577 keV and the incident beam size was 0.5×0.5 mm^2. The sample mounted on an eight-circle diffractometer was aligned first for the symmetric Bragg reflection GaAs(006), the primary reflection G, by adjusting the Bragg angle $\theta = 36.492°$.[20] The crystal is then rotated around the normal of the G-reflecting planes (the reciprocal lattice vector $\mathbf{G}$), the azimuthal ϕ scan, to bring the additional set of atomic planes $L(=(1-13))$, the secondary reflection, also satisfying Bragg's law. Two diffracted waves along the wave vectors $\mathbf{K}_G$ and $\mathbf{K}_L$ are generated by the G and L reflections for an incident (000) wave $\mathbf{K}_O$ simultaneously [Fig. 1(a)]. The latter (1−13) is a surface diffraction, because the reciprocal lattice point L lies on the equatorial plane of the Ewald sphere [Fig. 1(b)] parallel to the crystal surface. All the reciprocal lattice points, O(000), G(006), and L(1−13), lie simultaneously on the surface of the Ewald sphere of the radius equal to $1/\lambda$ [Fig. 1(b)].

The surface diffracted (1−13) wave, making 37.654° in ϕ from the plane of incidence of the (006), was monitored by a scintillation counter and an image plate (IP) placed 30 cm away. $\phi = 0°$ is the angle at which the [110] lies in the plane of incidence. One pixel in the IP corresponds to 0.1 mm. The diffraction intensity profiles of the (006) and (1−13) versus

a)Author to whom correspondence should be addressed; electronic mail: slchang@phys.nthu.edu.tw

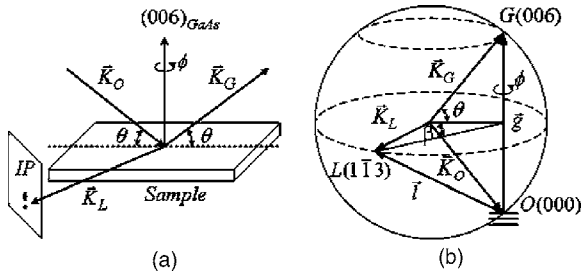

FIG. 1. Bragg-surface diffraction geometry for GaAs(006)/(1−13): (a) in real space and (b) in reciprocal space.

θ and ϕ (not shown), respectively, were measured by the counter. Images of the surface diffracted waves at different ϕ were recorded for the incident x-ray wave hit the center of the sample. In principle, for a fixed θ, the surface diffraction images taken at varying ϕ should provide the information about lattice-constant variation parallel to the interface. For fixed ϕ, the surface diffracted images taken at various θ yield the information about lattice-constant variation normal to the interface. Figure 2(a) shows the surface (1−13) diffraction images obtained for increasing ϕ in a step of 0.02° at θ =36.492°, where the intensity of (006) is maximum. The lower tiny spot is the image of the Bragg-surface diffracted (1−13) beam from the deep GaAs lattice, and the upper rather diffuse spot is due to the specular reflection from an isostrained layer near the interface.[13] The contribution of the diffraction from the gold film is negligibly small due to large lattice mismatch with GaAs. For a fixed θ angle the vertical separation between the two images decreases when the angle ϕ increases. This is schematically shown in Fig. 2(b), where C are the positions of maximum diffuse intensities for a ϕ angle. Point A represents the tiny diffraction spot from the deep substrate. The vertical angular separation ξ between the diffuse maximum C and spot A increases, when the ϕ angle decreases. Meanwhile spot A also shifts horizontally to D [Fig. 2(c)]. We also detected that at a fixed ϕ the sharp substrate spot A moves upward to E for increasing θ angles. The vertical movement of the diffuse spot for varying ϕ angles

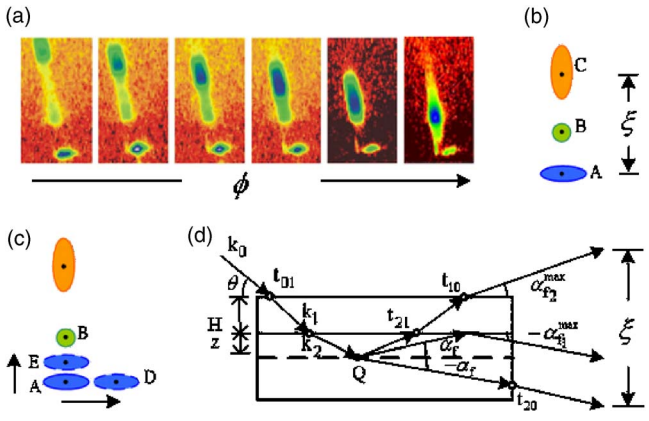

FIG. 2. (a) Diffraction images of GaAs(1−13) vs ϕ (ϕ=37.554° for the first image, 0.02° per step in ϕ). (b) Schematic of the diffuse surface scattering images from the interface and the GaAs diffraction spot A. B is the interfacial diffraction spot due to internal total reflection and C is the maximum of the diffuse images at a given ϕ angle. (c) The movements of spot A, A→D and A→E, for varying ϕ and θ, respectively. (d) Scattering processes involved in a thin film of thickness H and an isostrained layer of depth z below the interface. t is the transmission function. Subscripts 0, 1, and 2 mean the air, film, and isostrained layer, respectively.

can be considered as scattering of the surface diffracted wave from an isostrained layer at different depths normal to the interface, as was described for scattering from quantum dots.[13] Namely, the ϕ angle is associated with the depth at which an isostrained layer is located.

Referred to Refs. 13–15, the generalized structure factor describing the diffuse scattering can be derived for our case, where the incident angle θ is larger than the critical angle α_c of total external reflection, and the exit angle of the surface diffracted beam is close to α_c. For a plain interface, the structure factor of the sample is proportional to the product of the transmission functions of the Fresnel formula in terms of the incident/scattering angle $\alpha_{i,j}$. It describes the changes in field strength as the beam enters and exits the sample through the surface and interface. For a strained interface, the optical part of the scattering process includes additional multiple scattering between the surface and the interfaces. Figure 2(d) shows schematically the scattering processes in a thin film/substrate, where H and z are, respectively, the thickness of the film and the vertical penetration depth of x rays in the isostrained substrate layer. The incoming beam passes through two interfaces via refraction. The refracted beam is then surface diffracted by the total momentum transfer $\mathbf{Q}=2\pi\mathbf{l}$ introduced from a particular region of constant lateral lattice parameter at penetration depth z below the interface. After Q, a surface diffracted beam and its conjugated surface specularly reflected diffuse beams are produced from the substrate and the strained layer, respectively. The former goes through the substrate and exits from the side of the crystal. The latter is refracted first by the substrate/film interface and then by the film/air interface. If the refractive index of the strained layer is larger than that of the thin film, then total internal reflection occurs for a diffuse beam of the incident angle equal to α_c, which produces an additional beam along the interfacial direction [image B in Fig. 2(b)]. Otherwise, there is no additional interfacial beam produced. $\theta=\alpha_i$ is the incident angle and α_f is the grazing exit angle at point Q. From the position $\alpha_f^{\max}$ of the pronounced maximum, the depth z can be determined by

$$z=\begin{cases}\dfrac{1}{2k_2\alpha_{f1}^{\max}}\left[2\pi-k_1H-\cos^{-1}\left(\dfrac{\alpha_{f1}^{\max}}{\alpha_c}\right)\right] & \text{for } \alpha_f<\alpha_c\\ \dfrac{1}{2k_2\alpha_{f2}^{\max}}[2\pi-k_1H] & \text{for } \alpha_f\geqslant\alpha_c,\end{cases} \tag{1}$$

where k is the modulus of the wave vector of the incoming beam at the substrate. The first relation is valid for a total internal reflection to occur. From the second relation, the penetration depth z can be determined from the ξ angle as $\alpha_{f2}^{\max}+\alpha_f=\xi$. Experimentally, ξ can be measured, so can the depth z.

On the other hand, the vertical and horizontal shifts of spot A [Fig. 2(c)] are closely related to the lattice-constant variation of GaAs perpendicular and parallel to the interface, respectively. These variations can be determined by considering the geometric condition for a general three-wave (O,G,L) diffraction [Fig. 1(b)],[20]

$$\Delta l_\perp=\frac{1}{\lambda}\cos\theta\Delta\theta, \tag{2}$$

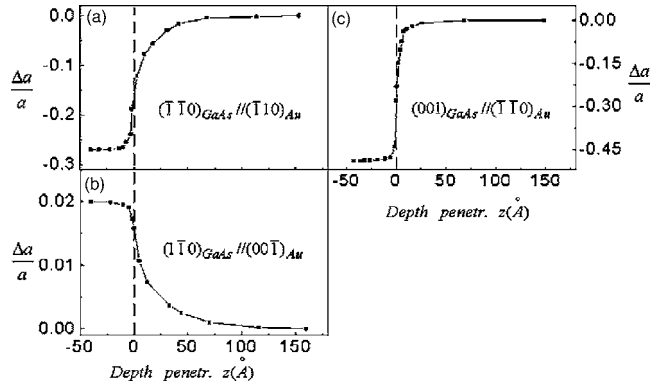

FIG. 3. Lattice-constant variations and strains parallel and perpendicular to the interface with respect to the x-ray penetration depth. $z \leqslant 0$: the Au thin film; $z \geqslant 0$: the GaAs substrate. The resolution in depth is 2.0 Å.

$$\Delta l_{\parallel} = \frac{2l_{\parallel}^2\sqrt{(1/\lambda)^2-(g/2)^2}}{l_{\perp}^2 - l_{\parallel}^2 - l_{\perp}g}\left[\sin\beta\Delta\phi + \frac{(l_{\parallel}^2+l_{\perp}^2)(g/4)-l_{\perp}(1/\lambda)^2}{2l_{\parallel}^2[(1/\lambda)^2-(g/2)^2]^{3/2}}\frac{2}{\lambda}\cos\theta\Delta\theta\right], \tag{3}$$

where $l_{\perp}$ and $l_{\parallel}$ are the components of the reciprocal lattice vector $\mathbf{l}$ perpendicular and parallel to the interface, i.e., $\mathbf{l}_{\perp}$ is parallel to $\mathbf{g}$. β is the angle between $l_{\perp}$ and the plane of incidence of the G reflection [Fig. 1(b)], which is related to ϕ, i.e., $\Delta\phi = \Delta\beta$.

Using the positions of diffraction spots, especially the shifts $A \rightarrow D$ and $A \rightarrow E$ [see Fig. 2(c)], at various θ and ϕ, two-dimensional lattice-constant variations and strains along $[1-10]$ near the interface can be determined. Also a ϕ angle gives the information about the depth z of an isostrained layer which satisfies the surface L diffraction condition. Moreover, when ϕ is rotated 90° from $\phi = 37.654°$, the three-wave (000)(006)(−1−13) Bragg-surface diffraction occurs. We can use that diffraction and repeat the same procedure. The lattice-constant variation along $[-1-10]$ can be determined. Thus we have three-dimensional information about the interface strains, i.e., $\Delta S_{\perp} = \Delta l_{\perp}/l$, $\Delta S_{\parallel} = \Delta l_{\parallel}/l$, and the strain normal to the interface.

For the Au film, as usual we employed the conventional grazing-incidence x-ray diffraction (GIXD) and Bragg diffraction to measure lattice-constant variations. Au(−220) and Au(004) in-plane reflections and Au(−2−20) Bragg reflection were used for estimating the lattice variations in the two in-plane directions and the normal to interface, respectively. From the observed diffraction spots at different azimuth angles ϕ and Bragg angles θ, the variations of lattice constant at different heights from the interface, like that in quantum dots, were determined according to Bragg's law. The results are combined into Fig. 3.

Figures 3(a)–3(c) show the strains along the directions GaAs$[-1-10]$ and GaAs$[1-10]$ parallel and GaAs[001] normal to the interface for both the Au film and GaAs substrate as functions of the depth z. $z \leqslant 0$ is the Au thin film and $z \geqslant 0$, for the GaAs substrate. Similar to the structure of a quantum dot, the strained substrate crystal near the interface can be considered as an ensemble of isostrained layers with different strains in a different layer. The closer the layer to the interface is, the larger the strain. Figures 3(a) and 3(b) are obtained from the measurements of three-wave Bragg-surface diffractions, (000)(006)(−1−13) and (000)(006)(1−13), together with Au (−2−20) and (2−20) GIXD, respectively. The lattice distortions occur in the range from 65 Å in the substrate below the interface to 7 Å in the film above the interface. The distortion about −27% with respect to GaAs along GaAs$[-1-10]$ is of one order of magnitude larger than that (2%) along GaAs$[1-10]$ Figure 3(c) is obtained from GaAs(600) and Au(−2−20) Bragg reflections. The lattice-constant variation about −49% with respect to GaAs normal to the interface is rather abrupt, which occurs about 10 Å in the substrate below and 8 Å in the film above the interface [Fig. 3(c)].

We have also applied this BSD method to the sample system of $Sc_2O_3/Si(111)$, where the refractive index of Sc_2O_3 is larger than of Si. The strain field exists up to 10 Å from the interface in the Sc_2O_3 film. There is no strain detected in the substrate. This result is consistent with other measurements.[21]

In conclusion, we have demonstrated an x-ray diffraction method, which is capable of determining strain field of interfaces in epilayer/crystal sample systems. This generic method can be equally applied to other nanoscale single-crystal sample systems, such as thin films, multilayers, quantum dot, etc., of any combinations in refractive indices, without invoking total reflection.

The authors thank H.-Y. Lee of the NSRRC and Y.-R. Lee of NTHU for technical supports and discussion. The financial support from NSC of Taiwan, Republic of China, is also gratefully acknowledged.

[1] J. Stangl, V. Holy, P. Mikulyk, and G. Bauer, Appl. Phys. Lett. **74**, 3785 (1999).
[2] M. Rauscher, R. Paniago, H. Metzger, Z. Kovats, J. Domke, and J. Peisl, J. Appl. Phys. **86**, 6763 (1999).
[3] L. H. Avanci, L. P. Cardoso, S. E. Girdwood, D. Pugh, J. N. Sherwood, and K. J. Roberts, Phys. Rev. Lett. **81**, 5426 (1998).
[4] M. A. Hayashi, S. L. Morelhao, L. H. Avanci, L. P. Cardoso, M. Sasaki, L. C. Kretly, and S. L. Chang, Appl. Phys. Lett. **71**, 2614 (1997).
[5] D. Y. Noh, Y. Hwu, H. K. Kim, and M. Hong, Phys. Rev. B **51**, 4441 (1995).
[6] J. Wang, M. J. Bedzyk, and M. Caffrey, Science **258**, 775 (1992).
[7] S. Di Fonzo, W. Jark, S. Lagomarsino, C. Giannini, L. De Caro, A. Cedola, and M. Muller, Nature (London) **403**, 638 (2000).
[8] Q. Shen and S. Kycia, Phys. Rev. B **55**, 15791 (1997).
[9] A. Broadhurst, K. D. Rogers, T. W. Lowe, and D. W. Lane, Acta Crystallogr., Sect. A: Found. Crystallogr. **A61**, 139 (2005).
[10] C.-H. Hsu, H.-Y. Lee, Y.-W. Hsieh, Y. P. Stetsko, M.-T. Tang, K. S. Liang, N. T. Yeh, J.-I. Chyi, and D. Y. Noh, Physica B **336**, 98 (2003).
[11] R. Feidenhans'l, Surf. Sci. Rep. **10**, 105 (1989).
[12] I. K. Robinson and D. J. Tweet, Rep. Prog. Phys. **55**, 599 (1992).
[13] I. Kegel, T. H. Metzger, A. Lorke, J. Peisl, J. Stangl, G. Bauer, J. M. García, and P. M. Petroff, Phys. Rev. Lett. **85**, 1694 (2000); I. Kegel, T. H. Metzger, A. Lorke, J. Peisl, J. Stangl G. Bauer, K. Nordlund, W. V. Schoenfeld, and P. M. Petroff, Phys. Rev. B **63**, 035318 (2001).
[14] M. Kimura, A. Acosta, H. Fujioka, and M. Oshima, J. Appl. Phys. **93**, 2034 (2003).
[15] H. Dosch, *Critical Phenomena at Surfaces and Interfaces: Evanescent X-Ray and Neutron Scattering* (Springer, New York, 1992).
[16] H. Baltes, Y. Yacoby, R. Pindak, R. Clarke, L. Pfeiffer, and L. Berman, Phys. Rev. Lett. **79**, 1285 (1997).
[17] P.-C. Wang, G. S. Cargill III, I. C. Noyan, and C.-K. Hu, Appl. Phys. Lett. **72**, 1296 (1998).
[18] A. Armigliato, R. Balboni, A. Benedetti, S. Frabboni, A. Tixier, and J. Vanhellemont, J. Phys. III **7**, 2375 (1997).
[19] A. J. Wilkinson, Ultramicroscopy **62**, 237 (1996).
[20] S.-L. Chang, *X-Ray Multiple-Wave Diffraction: Theory and Application* (Springer, Berlin, 2004).
[21] M. Hong, A. R. Kortan, P. Chang, Y. L. Huang, C. P. Chen, H. Y. Chou, H. Y. Lee, J. Kwo, M. W. Chu, C. H. Chen, L. V. Goncharova, E. Garfunkel, and T. Gustafsson, Appl. Phys. Lett. **87**, 251902 (2005).